Source/Load Pull Investigation of AlGaN/GaN Power Transistors with Ultra-High Efficiency

V. Carrubba, R. Quay, S. Maroldt, M. Mußer, F. van Raay, and O. Ambacher

Fraunhofer Institute for Applied Solid State Physics (IAF), Tullastrasse 72, 79108, Freiburg, Germany

vincenzo.carrubba@iaf.fraunhofer.de

Abstract — **This paper presents the investigation of highly performing AlGaN/GaN HEMT power transistors through source-pull and load-pull analysis using an active harmonic load-pull system. The advantages of the GaN technology together with the right terminations lead to power transistors with promising output power and efficiency. When setting properly the first three output terminations, a drain efficiency as high as 84.3% has been achieved at 2 GHz while delivering 4.3 W of output power for a 1.2 mm device gate width. However, it has been seen that the achievement and the set of the optimum output terminations do not lead to the best device performance. When presenting such three optimum output impedances together with the proper *second harmonic source* termination, it has been demonstrated that higher drain efficiency up to 88% can be obtained delivering output power as high as 4.4 W and a power gain of 14.9 dB. Indeed the GaN HEMT used in this work has reached record peak drain efficiency of 90% delivering output power of 3.5 W.**

Index Terms— **Aluminum gallium nitride, high efficiency, microwave measurements, power amplifiers, power transistors.**

I. INTRODUCTION

POWER AMPLIFIER designs used in wireless communication networks are becoming more and more sophisticated in order to meet the modern requirements. Among the various PA output specifications, one of the most important parameter is still the efficiency. High efficiency means low power consumption and therefore less power dissipated in the environment. In the last decades various PA high efficiency classes have been studied, starting from the more standard class-AB [1-3] going through the switch modes Class-D and Class-E [1-7] to the harmonically tuned modes Class-F and Inverse Class-F [1-3, 8-9]. In these cases the high harmonics can be properly set in order to increase the PA efficiency and therefore minimize the overall power consumption. However, in order to reach certain performances at the PA stage, the device itself and therefore the adopted technology plays a key role in the overall output performance. This paper will show an harmonic load/source pull analysis based on the in house (IAF) highly performed 250 nm AlGaN/GaN power transistors [10-12] for which very high drain efficiency is achieved.

II. ALGAN/GAN TECHNOLOGY

The device used in this work is a HEMT (High Electron Mobility Transistor) power transistor in AlGaN/GaN technology grown on a 3-inch semi-insulating SiC (Silicon Carbide) substrate [10-12] with the photo shown in Fig. 1.

The epitaxy of the AlGaN/GaN heterostructure is carried out using multi-wafer metal organic chemical vapor deposition (MOCVD). In particular the frontside processing involves alloyed Ti/Al/Ni/Au ohmic contacts, implantation isolation and SiN passivation assisted T-gates processed by using E-beam lithography as well as a source terminated field plate. Here the device is fabricated with a gate length of L_G=250 nm and a gate width of W_G=1.2 mm (6x200 μm) optimized for high gain, high power density as well as very high efficiency.
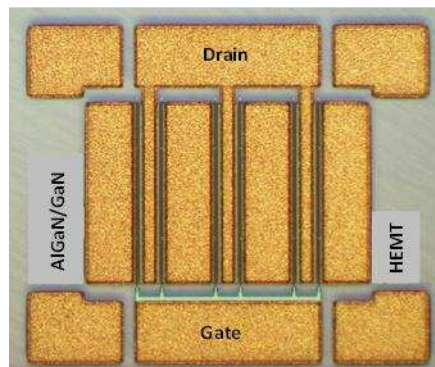

Fig. 1. Microscope photograph of the IAF 1.2 mm AlGaN/GaN HEMT power transistor.

III. LOAD PULL EXPERIMENTAL INVESTIGATION: $Z_{L,F0}, Z_{L,2F0}, Z_{L,3F0}$

The experimental measurements have been conducted on the 1.2 mm AlGaN/GaN power device described in Section II at 2 GHz of operating fundamental frequency, drain bias voltage V_{DS} = 30 V and gate bias voltage V_{GS} = V_{TH} = -2.2 V (pinch-off). The measurement system used for testing the GaN device and validate the experiment is an active harmonic

load-pull system based on a four coupler configuration that allows the simultaneous measurement of the input and output reflection coefficients at the DUT (device under test) reference plane, with the simplified block diagram shown in Fig 2. The measurement system is capable of controlling three tuning loops (derived from the fundamental input) meaning that three terminations can be properly controlled and set both in terms of magnitude and phase. More details of the active harmonic load-pull system can be found in [13-14].
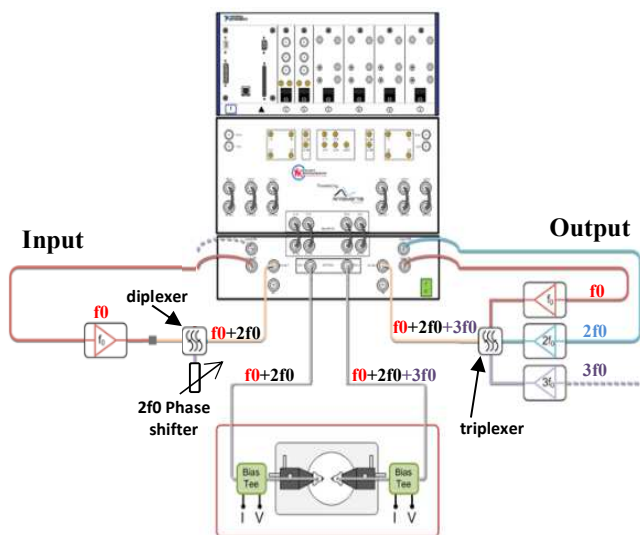

Fig. 2. Simplified block diagram of the active harmonic load-pull system [14].

First of all the input power together with the fundamental impedance are swept in order to find the first optimum condition in the Class-B like case, while keeping the second and third harmonic terminations at around 50 Ω. Although the high harmonic terminations are still not optimized (but kept at 50 Ω) high drain efficiency DE between 65% and 68% and power gain G greater than 15 dB while delivering high output power between around 4 W and 8 W are already achieved as shown in Fig. 3.
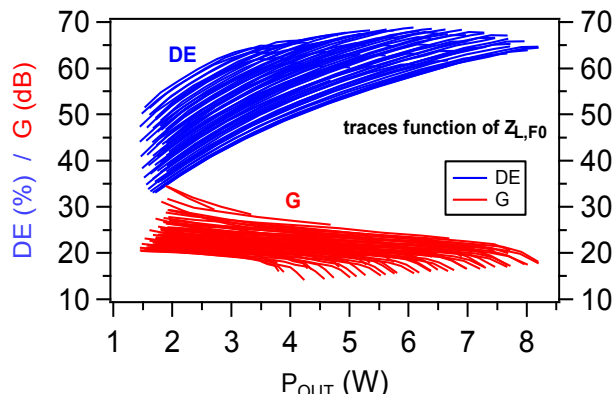

Fig. 3. DE and G function of $Z_{L,F0}$ and P_{OUT} with the higher harmonics set to the system 50 Ω impedance.

Once the fundamental impedance has been optimized, the second and third harmonic terminations have been both swept around the edge of the Smith chart [15-16]. Best trade-off

performance is delivered for $Z_{L,F0}$=140+j92 Ω, $Z_{L,2F0}$=1+j100 Ω and $Z_{L,3F0}$=0+j0 Ω (short-circuit), with the performance shown in Fig. 4 and 5. In this case the drain efficiency varies between DE=85.5% where output power P_{OUT}=3.6 W and DE=76.9% where P_{OUT}=7.6 W. As noted and as expected, power and efficiency are inversely proportional; the highest power is accompanied with the lowest efficiency and vice-versa. In this case, for the 1.2 mm gate width device at f=2 GHz and for V_{DS}=30 V, P_{OUT}=4.3 W (P_{OUT}=3.6 W/mm) is a satisfactory delivered output power accompanied with a very high drain efficiency of DE=84.3% and a power gain of G=14.5 dB, as highlighted in red in Fig. 4. Furthermore, high PAE=81.3% and transducer power gain G_T=10.7 dB are shown in Fig. 5. In this case both fundamental and second harmonic "*source*" impedances are set to around the 50 Ω of the system impedance.
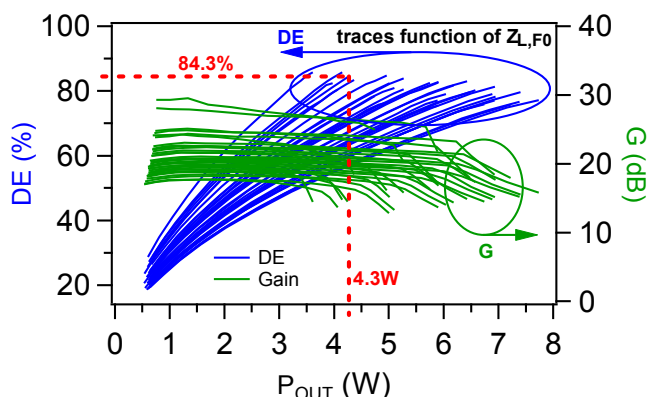

Fig. 4. DE and G as a function of $Z_{L,F0}$ and P_{OUT} for optimum $Z_{L,2F0}$ and $Z_{L,3F0}$.
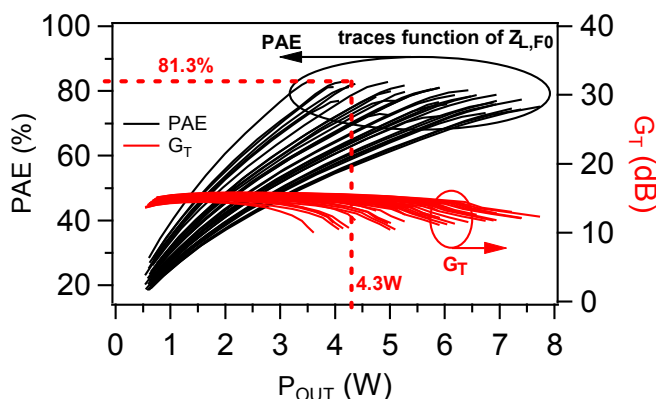

Fig. 5. PAE and G_T as a function of $Z_{L,F0}$ and P_{OUT} for optimum $Z_{L,2F0}$ and $Z_{L,3F0}$.

IV. LOAD/SOURCE PULL EXPERIMENTAL INVESTIGATION: $Z_{L,F0}$, $Z_{L,2F0}$, $Z_{L,3F0}$ AND $Z_{S,2F0}$

Despite the measurement system used for the characterization of the GaN device can control "only" 3 tuning loops, an additional phase shifter has been added in the input path (also shown in Fig. 2) in order to also control the "*second harmonic source*" impedance. Therefore, in this case, three terminations in the output ($Z_{L,F0}$, $Z_{L,2F0}$, $Z_{L,3F0}$) as well as the second harmonic termination in the input ($Z_{S,2F0}$) can be controlled. It is however important to highlight that while the three terminations in the output can be controlled both in

terms of magnitude and phase and thus set anywhere in the Smith chart, the second harmonic in the input can only be controlled in terms of phase while presenting similar magnitude of around 0.35.

Fig. 6 shows the Smith chart with the optimum three load terminations achieved in Section III as well as the variation of the second harmonic source termination (black crosses) with magnitude between 0.3 and 0.4 as a function of different phases. The fundamental source impedance $Z_{S,F0}$ is around the 50 Ω system impedance.
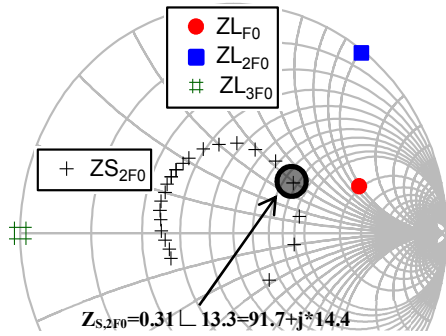

Fig. 6. Smith chart showing optimum $Z_{L,F0}$, $Z_{L,2F0}$ and $Z_{L,3F0}$ as well as the various $Z_{S,2F0}$.

The output performance related to the impedances of Fig. 6 is shown in Fig. 7. As it can be noted, the efficiency decreases with increasing the phase of $Z_{S,2F0}$, down to DE=82.7% where the $Z_{S,2F0}$ phase is equal to 200°. Amount the various $Z_{S,2F0}$ loads, the highest efficiency DE=86.8% with PAE=84% as well as P_{OUT}=4.5 W, G=14.9 dB and G_T=10.7 dB is achieved at $Z_{S,2F0}$=0.31∟13.3 (load also highlighted in black in Fig. 6).

For the different $Z_{S,2F0}$ phases both the output power as well as the large signal power gain G and transducer power gain G_T are quite similar, i.e. around 4.3-4.5W, 14.2-14.9 dB and 10.6-10.8 dB, respectively.
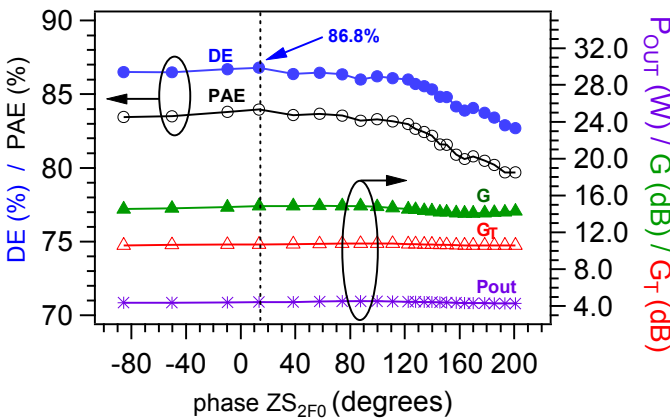

Fig. 7. DE, PAE, P_{OUT}, G and G_T function of the phase of $Z_{S,2F0}$ with magnitude of ≈ 0.3-0.4.

Finally, once the optimum second harmonic source impedance $Z_{S,2F0}$ is revealed, a final fundamental load-pull $Z_{L,F0}$ sweep is conducted in order to find the optimum final performance, as shown in Fig. 8 and 9. From Fig. 8, when considering the same output power of around 4.4 W

(≈ 3.7 W/mm), a drain efficiency of 88% is achieved. However, if considering lower output power of 3.6 W (3 W/mm), ultra-high drain efficiency of 90% is revealed which to the authors´ knowledge is the highest efficiency reported for AlGaN/GaN HEMTs at 2 GHz of frequency for output power of around 3 - 4 W. In this case PAE, power gain G and transducer power gain G_T of 86.7%, 14.3 dB and 10 dB have been measured, respectively.
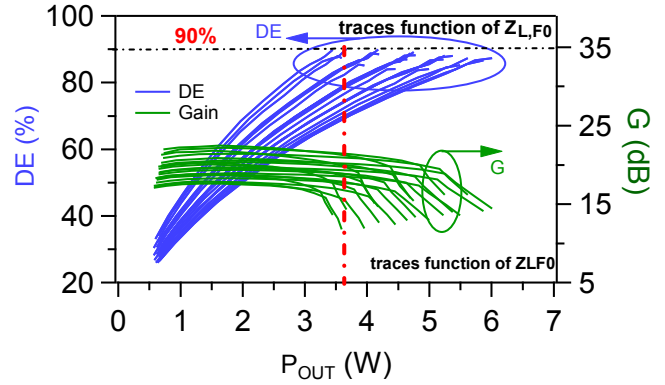

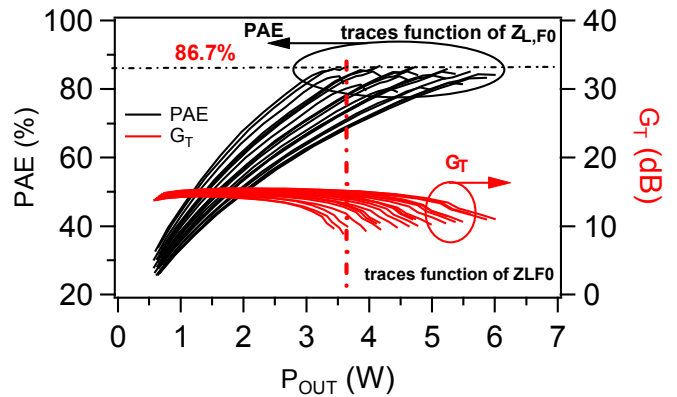Fig. 8. DE and G function of P_{OUT} for optimum $Z_{L,F0}$, $Z_{L,2F0}$, $Z_{L,3F0}$, $Z_{S,2F0}$.

Fig. 9. PAE and G_T function of P_{OUT} for optimum $Z_{L,F0}$, $Z_{L,2F0}$, $Z_{L,3F0}$, $Z_{S,2F0}$.

The drain voltage and current waveforms related to the highest measured 90% drain efficiency at both the device extrinsic plane (dotted lines) and the device intrinsic plane (solid lines) after de-embedding the effective output capacitance $C_{DS}+C_{GD}$=0.34 pF are shown in Fig. 10. Noted that while the voltage waveforms at the intrinsic and extrinsic planes are equals (solid and dotted red traces on top of each other) the current waveform behavior is affected from the output capacitance leading to negative values for the extrinsic waveform and to a more ideal compressed square-like waveform for the intrinsic plane. This can also been observed from the load-line of Fig. 11.

As for the waveforms, in the loadline behavior negative values of the drain current are observed for the extrinsic load-line (green line) for low values of drain voltages. Furthermore, it should be noted that despite the device is biased at V_{DS}=30 V, the maximum peaking voltage is around 90 V. This high peak is due to the fact that the second harmonic load termination presents a phase different from zero (Fig. 6) leading to the inverse Class-F like waveforms [9].

The very high efficiency condition is achievable thanks to the very low V_{knee} value of around 1-2 V as illustrated in the DCIV/loadline of Fig. 11. However, it is important to highlight that the maximum drain current achievable for this power transistor is around 1-1.2 A for which higher output power in the order of > 8 W can be achieved. On the other hand, in the high efficiency case, the loadline reaches its peak current at around 0.3-0.4 A which in this case is a satisfactory compromise in terms of very high efficiencies (DE>85%) accompanied with high output power (P_{OUT}>3.5 W) for the 1.2 mm AlGaN/GaN HEMT.
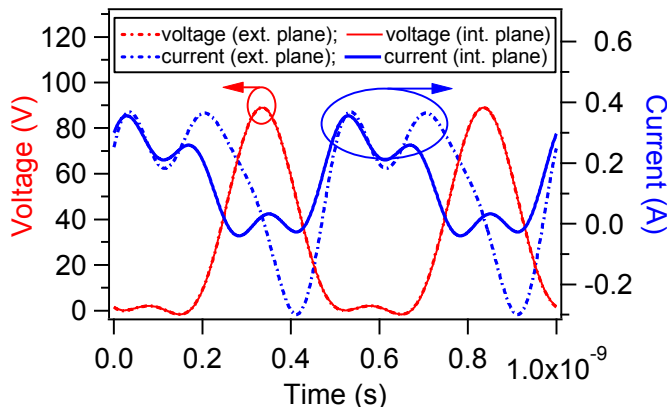

Fig. 10. Drain voltage and current waveforms at the extrinsic (dotted lines) and intrinsic (solid lines) planes related to the DE=90% terminations.
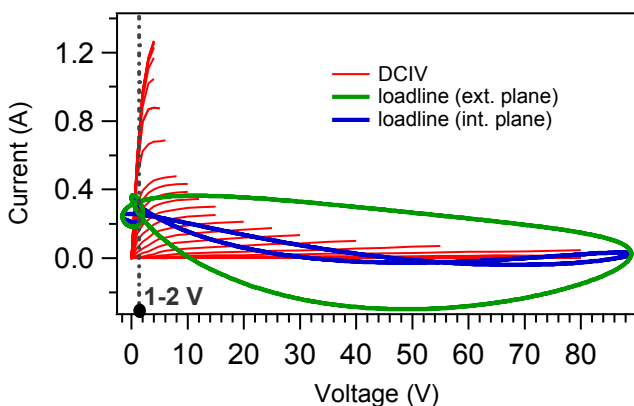

Fig. 11. DCIV and loadline at the extrinsic (green line) and intrinsic (blue line) planes related to the DE=90% highest efficiency state.

V. Conclusion

This paper has presented the analysis and investigation of an AlGaN/GaN HEMT power transistor with a gate length of 250 nm. The advanced GaN technology together with a high number of harmonic investigation through an active harmonic load-pull system shows that very high drain efficiency power transistors in the range of 85% can be achieved delivering high output power of 3.6 W/mm and gain of around 15 dB at 2 GHz of fundamental frequency. Furthermore, it has been demonstrated that by proper second harmonic source manipulation higher efficiency in the order of 88% can be revealed without trading off the initial output power and thus

still delivering 3.7 W/mm as well as similar gain of 14-15 dB. Once the optimum trade-offs of power, efficiency and gain are accomplished, the device has been run in its highest efficiency state. In this case lower output power of 3 W/mm is delivered with record peak efficiency of 90%.

References

[1] A. Grebennikov, N. O. Sokal, "Switchingmode RF Power Amplifiers," Linacre House, Jordan Hill, Oxford OX2 8 DP, UK, 2007.

[2] Steve. C. Cripps, "RF Power Amplifiers for Wireless Communications", 2nd Edition, Artech House Publishers Inc., ISBN: 0-89006-989-1, 2006.

[3] P. Colantonio, F. Giannini, E. Limiti, "High Efficiency RF and Microwave Solid State Power Amplifier," John Wiley & Sons Ltd, 2009.

[4] Lin Song, A. E. Fathy "A 20 W GaN HEMT VHF/UHF Class-D power amplifier," *Wireless and Microwave Technology Conference (WAMICOM)*, pp. 1-4, 2011.

[5] N. Sokal, A. Sokal, "Class E – A new class of high-efficiency tuned single-ended switching power amplifiers," IEEE Journal on Solid-State Circuits, Vol. SSC-10, pp. 168-169, March 1975.

[6] P. Sochor, S. Maroldt, M. Musser, H. Walcher, D. Kalim, R. Quay, R. Negra "Design and realisation of a 50 W gaN class-E power amplifier," *Asia Pacific Microwave Conference (APMC)*, pp. 518-521, 2011.

[7] M. P. van der Heijden, M. Acar, J. S. Vromans, "A compact 12-Watt high-efficiency 2.1-2.7 GHz class-E GaN HEMT power amplifier for base stations," *IEEE Microwave Symposium Digest (IMS)*, pp. 657-660, 2009.

[8] D. Schmelzer, S. I. Long "A GaN HEMT Class-F Amplifier at 2 GHz With > 80% PAE," *IEEE Journal of Solid State Circuits*, Vol. 42, pp. 2130-2136, October 2007.

[9] P. Wright, A. Shiekh, C. Roff, P. J. Tasker, J. Benedikt, "Highly efficient operation modes in GaN power transistors delivering upwards of 81% efficiency and 12W output power," *IEEE MTT-S Microwave Symposium Digest*, pp. 1147-1150, 2008.

[10] M. Dammann, M. Cäsar, P. Waltereit, W. Bronner, H. Konstanzer, R. Quay, S. Müller, M. Mikulla, O. Ambacher, P. van der Wel, T. Rödle, R. Behtash, F. Bourgeois, and K. Riepe, "Reliability of AlGaN/GaN HEMTs under DC- and RF-operation," in *Reliability of Compound Semiconductors Digest (ROCS)*, 2009, pp. 19-32.

[11] P. Waltereit, W. Bronner, R. Quay, M. Damman, R. Kiefer, W. Pletschen, S. Müller, R. Aidam, H. Menner, L. Kirste, K. Köhler, M. Mikulla, O. Ambacher," AlGaN/GaN epitaxy and technology," *International Journal of Microwave and Wireless Technology (IJMWT)*, pp. 3-11, 2010.

[12] P. Waltereit, W. Bronner, R. Quay, M. Damman, S, Müller, K. Köhler, M. Mikulla, O. Ambacher, L. Harm, M. Lorenzini, T. Rödle, K. Riepe, K. Bellmann, C. Bucheim, R. Goldhahn, "Development of rugged 2 GHz powerbars delivering more than 100 W and 60% power added efficiency," Physics Status Solid C 7, No. 10, pp. 2398-2403, 2010.

[13] M. Marchetti, M. J. Pelk, K. Buisman, W. C. E. Neo, M. Spirito " Active harmonic loadpull with realistic wideband signals," IEEE Transaction on Microwave Theory and Techniques, Vol. 56, No. 12, pp. 2979-2988. December 2008.

[14] Anteverta-mw website: http://www.anteverta-mw.com

[15] C. Roff, J. Benedikt and P. J. Tasker, "Design Approach for Realization of Very High Efficiency Power Amplifiers," *IEEE MTT-S Int. Dig.*, June 2007, pp. 143-146.

[16] A. L. Clarke, M. Akmal, J. Lees, P. J. Tasker, J. Benedikt, "Investigation and analysis into device optimization for attaining efficiencies in-excess of 90% when accounting for higher harmonics," *IEEE MTT-S* May 2010, pp. 1114-1117.